Performance Analysis of Hydraulic Machines Using Impellers Made from Conventional Steel and 3D Printing Co-polymer

Performance Analysis of Hydraulic Machines Using Impellers Made from Conventional Steel and 3D Printing Co-polymer

D Sitte and H Sutanto*

[1]Department of Mechanical Engineering, Faculty of Engineering, Czech University of Life Sciences Prague, Prague, Czech Republic
[2]Department of Mechanical Engineering, Faculty of Engineering, Atma Jaya Catholic University of Indonesia, Jakarta, Indonesia

*Corresponding author: hadi.sutanto@atmajaya.ac.id

Abstract. The research on hydraulic machines in industries is appropriate for many reasons. This paper deals with the creation of 3D prototypes of impellers of hydraulic machines printed from ABS plastic and verification of operating characteristics compared to conventional steel impellers of pump and also in turbine mode. The work includes properties, composition and verification of mechanical properties of ABS for different printing methods. Practical measurements of the specific geometry of the different 3D variants of the radial one-stage centrifugal impeller from ABS compared to metal wheels in the real hydraulic circuit are described. The results of the development of experiments demonstrate that the performance characteristics of the printed impellers of all variants have very similar functional values and very identical trends of functional curves of mechanical power and overall mechanical efficiency. At the same optimal speed, the highest performance and efficiency also as the metal wheels have been produced. It is clear from the results of work that prototypes produced by 3D printing achieve optimal performance parameter values in hydraulic testing and it is possible to successfully use this advanced technology in the verification of newly developed pumps, turbines and pumps turbines.

1. Introduction

Hydraulic machines, such as pumps and turbines are widely used in industrial and agricultural fields for irrigation and water supply [1]. In general, they have four different parts as suction and exit pipes, impellers and volute. The impeller is the core part and it converts the mechanical energy into pressure energy [2], which directly determine the transport capacity and the hydraulic performance of centrifugal pumps. It means that optimized design of impeller is essential and significant for the efficient operation of a centrifugal pump [3].

The use of 3D-CAD graphics systems is now a great tool for experiment, research and manufacturing activities in engineering. The basic principle is a parameterized graphical three-dimensional model in CAD software and now it can be used like CATIA V5, Creo, Inventor or SOLIDWORKS. Rapid Prototyping technology is one of the systems for creating faster and now affordable prototypes from 3D printers. The results are also the quality, possibilities and speed of 3D printed components to begin for replacing conventional ways of production itself [4].

Manufacturing companies offer a wide range of amateur and industrial 3D printers. In practice, the nomenclature of printing technology is based on the type of printing material such as powdered BJ

(Binder Jetting) and SLS (Laser Sintering), liquid SLA (Stereo Lithography) and rigid FDM (Fused Deposition Modelling). A common principle of production of a 3D printing component is the gradual addition of material by layer, as opposed to classical machining when the material is taken away by the subtractive processes. FDM technology was developed by Stratasys and it is the most widely used method of 3D printing of plastic components in engineering. For its positive properties, it was used in this work for making all functional prototypes on the 3D printer Dimension Elite Printer 180-00105 [5], [6].

Acrylonitrile-butadiene-styrene or ABS material, is an amorphous thermoplastic industrial co-polymer with a wide range of uses because of its universal properties. It is very well resistant to mechanical damage, impact and strain at low and high temperatures. ABS has considerable toughness and very good machinability. It is stable and resistant to UV radiation for a long time. ABS material is also low-soak, health-resistant and easy to withstand acids, hydrocarbons, hydroxides, oils and fats. On the contrary, it is very well soluble in acetone or in 1.2 dichloromethane. The ABS plus (ABS-P430 Model) variant, which has 40% higher strength than standard ABS, was used for printing in this particular case [7], [8], [9].

Verification of performance characteristics and operating parameters in the development, manufacture and supply of pumps is specified in ISO 9906. The standard specifies hydraulic power tests for all rotor dynamic pumps. And it can be used for pumps of all sizes and on which wheels pumped liquids that behave like pure cold water. Testing of the impellers used in the experiment was based on this standard [10].

The main purpose of this work is to verify the functional parameters and utility properties of a specific geometry of 3D printing plastic impellers prototypes compared to the parameters of the identical geometry of metal impellers produced by conventional technologies, such as metal casting, for pump and turbine mode during the dynamic load in the real hydraulic circuit.

2. Background Theory

2.1. Preparing a 3D model

The process of fast prototyping begins with creation of a 3D digital model in a CAD modelling program, here Inventor and Creo. Preparing a 3D model for printing begins with checking and editing geometry based on experience with a certain percentage of the shrinking of print dimensions, on modelling the necessary technological additions for clamping and machining. For functional impeller surfaces a machining allowance of 1 mm per radius was chosen, as seen in Figure 1. The following step was the conversion of a 3D digital model to Standard Tessellation Language (STL). The purpose was to create a sufficiently fine triangulation network that determines the resulting quality of the printed prototype, see Figure 2.

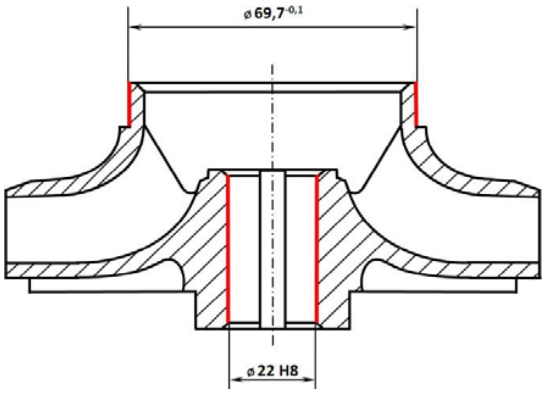

Figure 1. Working areas of the impeller.

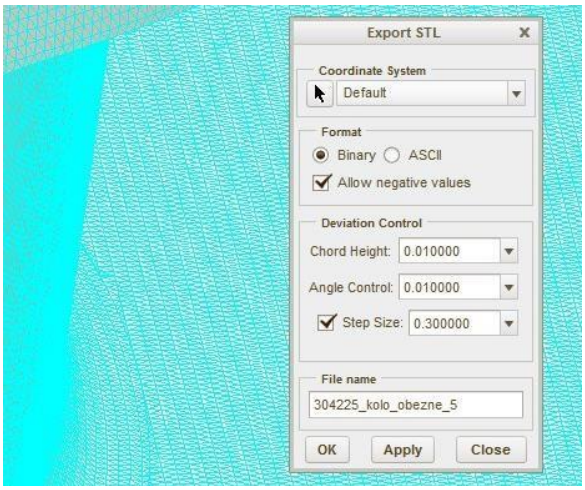

Figure 2. Creation of STL network.

The STL model was load into Grab-CAD Print. The orientation of the prototype on the print mat has been chosen, since the tensile strength is better in the direction of printed fibers than the strength perpendicular to the printed layers. The orientation of the part also affects the construction and consumption of supporting material (Figure 3). The position of the prototype on the mat affects the print temperature, which is important for test samples. In the following step, the print parameters were selected. The construction of the carrier material was related to the value of automatic construction (smart). The nature of the prototype construction was chosen depending on the printed variant, either for full material (solid) or shell structure with a honeycomb filling inside. The thickness of the print layers has always been set to 178 micrometers for softer and more precise printing. Figure 4 shows the simulation of automatic construction of the model and support material [11]. This process was followed by printing processes with parameters as in Table 1.

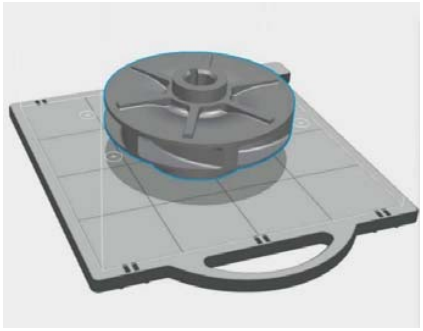

Figure 3. Position of the impeller on the mat [9]

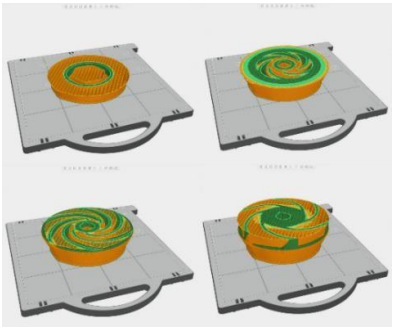

Figure 4. Simulation of the print job [9]

Table 1. The printing parameters [12].

Print job	Time (h:min:s)	ABS	Amount (cm³)	Support	Amount (cm³)
ABS full impeller	32:29:11	ABS-P430	187.5	P400SR	69.9
Composite impeller	30:57:01	ABS-P430	159.4	P400SR	72.7
ABS shell impeller	23:21:52	ABS-P430	87.9	P400SR	69.9

After printing process, the component was removed from the printer and left to cool naturally to room temperature. This was followed by rough cleaning of the supporting material, dimensional and visual inspection, softly cleaning in the SCA-1200 printer accessories in lye at 70°C. The cleaned part was washed with 70°C water and put in an ultrasonic bath, then was naturally dried at room temperature of 20°C. Now the prototype is in terms of printing completely finished and it can be proceed to the advanced machining. After machining, the process of component is already finish, and it remains to verify the appearance and required dimensions [8], [13].

2.2. Mechanical tests of ABS-P430 plastic

To verify the mechanical properties of printed ABS-P430 plastic, static load tensile tests have been established according to ISO 527-1 and ISO 527-2. The three sets of type A1 samples were tested after five pieces printed with different directions of printing fibers, see Figure 5. Samples were printed with consistent compliance using the same printing parameters as prototypes of the impellers were produced. The tests were carried out on the Instron 3382 test engine, see Figure 6. The test was controlled by a feed of 1 mm. min^{-1} and it was completed at the time of the sample infringement. Figure 7 shows a test sample which is captured in the detail of the breach [14], [15].

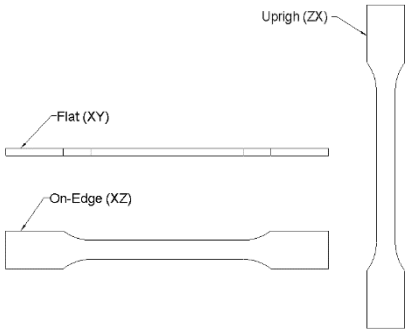

Figure 5. Test samples A1 [14].

Figure 6. The test machine.

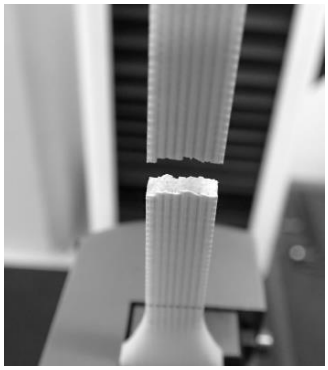

Figure 7. Test sample ZX.

2.3. Experimental verification of turbine and pump performance parameters

For laboratory verification, the geometry of the impeller was selected, which is displayed in the spiral cabinet together with the pump parameters as specified in Figure 8.

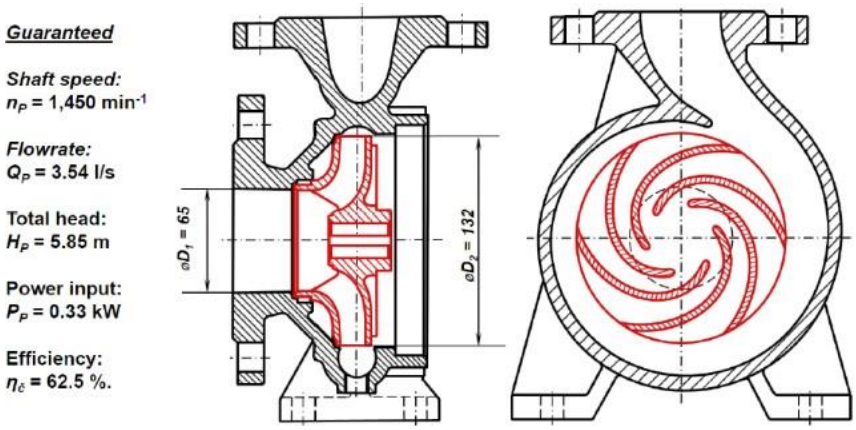

Figure 8. Metal impeller in spiral housing and pump parameters [15].

The radial one-stage centrifugal pump impellers produced by conventional casting methods (cast iron, stainless steel) and Rapid Prototyping technology with 3D printing technology have been tested. These wheels were tested in pump operation at 1,450 rpm.min^{-1} and 2,950 rpm.min^{-1} as well as in a turbine mode.

Impellers produced by Rapid Prototyping technology have been printed in three 3D printing variants, while consistently maintaining the conformity of all STL formation parameters, orientation, location, layer thickness and support creation. The experiments using the following 5 types of impellers:

- Steel impeller, **Figure 9**.
- Cast iron impeller, **Figure 10.**
- ABS full impeller made of solid, **Figure 11.**
- ABS shell impeller, solid surface and porous (honeycomb) interior. **Figure 12.**
- Composite impeller using ABS solid with glued metal disc, **Figure 13.**

Figure 9. Steel impeller

Figure 10. Cast iron impeller

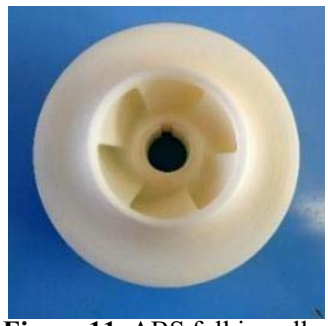

Figure 11. ABS full impeller

Figure 12. ABS shell impeller

Figure 13. Composite impeller

2.4. Hydraulic test circuit

A hydraulic test circuit was used to test the functional parameters of radial single-stage centrifugal impellers in pump and turbine mode. The diagram of the circuit for Figure 14.

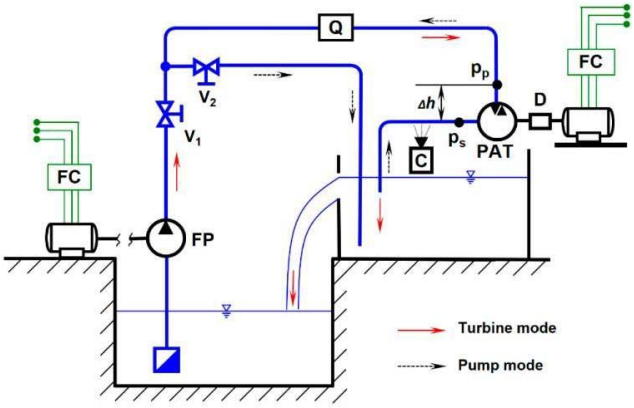

Q – flow meter, FP – power pump, PAT – tested pump or pump in turbine mode, V1, V2 – control valves, Pp, Ps – pressure sensors, D – dynamometer, FC – frequency converter, C – camcorder.

Figure 14. Hydraulic circuit scheme [16].

The hydraulic test circuit consists of two tanks, connecting pipes, control and measuring elements and the pump tested (P/T). By closing the V1 valve and regulating the V2 valve, water flows in the direction of the full arrows and forms a closed circuit for the tested pump. The pump was powered by a three-phase asynchronous electric motor with continuous shaft speed control using the LSLV0055s100- 4EOFNS frequency converter. The torque on the pump shaft was measured by the torque sensor (D) Magtrol TMB 307/41 (accuracy 0.1%). The water flow rate was measured using the electromagnetic flow meter (Q) SITRANS F M MAG 5100 W (accuracy 0.5%). Pressures in extrusion (p_p) and intake manifold (p_s) were measured by pressure sensors HEIM3340 (accuracy 0.5 %) installed according to the measurement requirement 1. accuracy class (ISO 9906).

The measurements were carried out with two constant speeds (1,450 rpm.min^{-1} or 2,950 rpm.min^{-1}) and set by the frequency converter. Gradually closing of the V2 valve increased the resistance of the discharge pipe. During the measurement, all values of the flow, engine speed, torque on the engine shaft, fluid pressures at the pump inlet and outlet were recorded.

The turbine operation of the pump took place on the same test line as follows. By closing valve V2 at the open valve V1, water flowed in the direction of intermittent arrows, and the power pump (FP) created hydro technical potential for the turbine. The measurement was carried out when the power pump (FP) was set up by the frequency converter to the required hydro technical potential. With this setting, the turbine was gradually braked using a three-phase electric motor with a frequency converter and braking resistors. The values of the flow, engine speed, torque on the engine shaft, fluid pressures at the pump inlet and outlet were measured and recorded. Declining hydro technical gradient with increasing turbine speeds was due to constant speeds of the power pump. To maintain a constant gradient, the power pump speed needs to be controlled, for example, by a frequency converter. The downward gradient was the same for all turbine variants and did not affect the measurement results. The same instruments were used for measurements as in pump operation, see Figure 15, Figure 16 and Figure 17 [10], [16].

Figure 15. Hydraulic circuit.

Figure 16. Detail of hydraulic circuit.

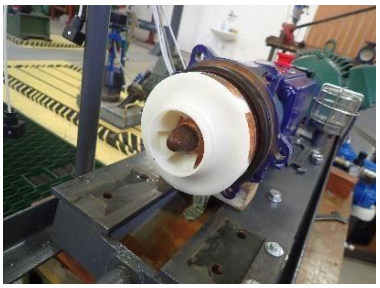

Figure 17. Composite impeller.

2.5. Calculation for pump and turbine

Pump mode:

- From Bernoulli's equation between intake (p_s) and displacement (p_p) of the pump and the continuity equation, the pump's variable energy was calculated as,

$$0 + \frac{p_s}{\rho} + \frac{v_s^2}{2} + Y_p = g.h + \frac{p_p}{\rho} + \frac{v_p^2}{2} \quad [J.kg^{-1}] \tag{1}$$

$$Q = v.S \qquad [m^3.s^{-1}] \tag{2}$$

$$Y_p = \frac{p_p - p_s}{\rho} + \frac{v_p^2 - v_s^2}{2} + g.h \qquad [J.kg^{-1}] \tag{3}$$

Turbine mode:

- From Bernoulli's equation between intake (p_{st}) and displacement (p_{pt}) of the turbine and continuity equation, the turbine's variable energy was calculated as,

$$0 + \frac{p_{st}}{\rho} + \frac{v_{st}^2}{2} + Y_t = g.h + \frac{p_{pt}}{\rho} + \frac{v_{pt}^2}{2} \quad [J.kg^{-1}] \tag{4}$$

$$Q_t = v_t.S \qquad [m^3.s^{-1}] \tag{5}$$

$$Y_t = \frac{p_{pt} - p_{st}}{\rho} + \frac{v_{pt}^2 - v_{st}^2}{2} + g.h \qquad [J.kg^{-1}] \tag{6}$$

Nomenclature

p – liquid pressure at a given location	[Pa]
ρ – specific mass of liquid	[kg · m^{-3}]
v – medium fluid speed at a given location	[m · s^{-1}]
Y_p – specific pump energy	[J · kg^{-1}]
Y_t – specific energy of the turbine	[J · kg^{-1}]
g – gravitational acceleration	[m · s^{-2}]
h – vertical lightness of pressure collection	[m]
Q – volumetric flow rate	[l · s^{-1}]
S – flow cross-section at a given location	[m^2]
d – the luminosity of the pipe at a given location	[m]

2.6. Test circuit input parameters

Pump mode:
- Intake manifold luminosity: d_s = 65 mm
- Extrusion pipe luminosity: d_p = 50 mm
- Vertical pressure relief: h = 290 mm

Turbine mode:
- Intake manifold luminosity: d_s = 50 mm
- Extrusion pipe luminosity: d_p = 65 mm
- Vertical pressure relief: h = 290 mm

3. Results and discussion

Test samples ABS-P430, see Figure 5, were tested in five pieces for each of the three directions of the printed fibers and reached the average tensile strength values in ZX = 14.8 MPa., XY= 26.8 MPa., and XZ = 29.9 MPa.

The measured and calculated values of pump and turbine mode have compiled with the performance characteristics of all impeller variants as shown in Figure 18 – 25. The pump mode experiments used two pump operation at speed 1,450 rpm.min^{-1} (see Figure 18 – 20) and 2,950 rpm.min^{-1} (see Figure 21– 23). Pump mode power characteristics at 1,450 rpm.min^{-1}

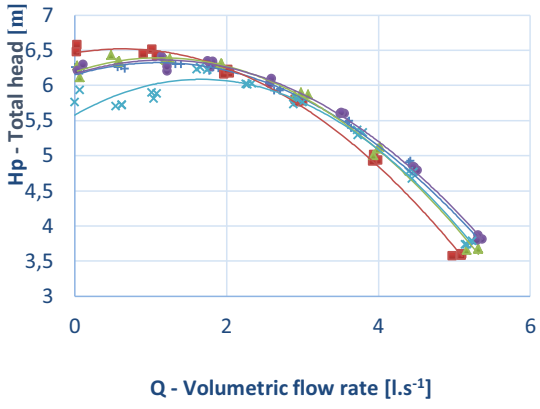

Figure 18. Total head vs flow rate

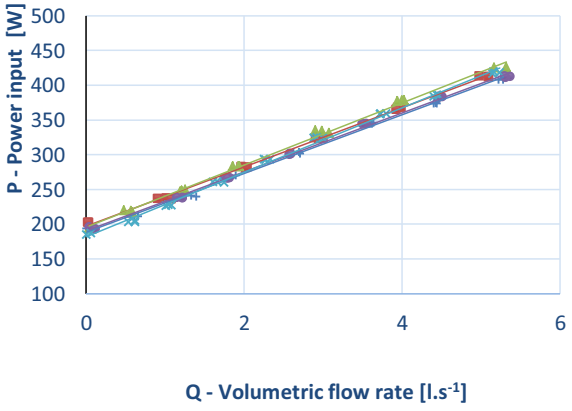

Figure 19. Power input vs flow rate

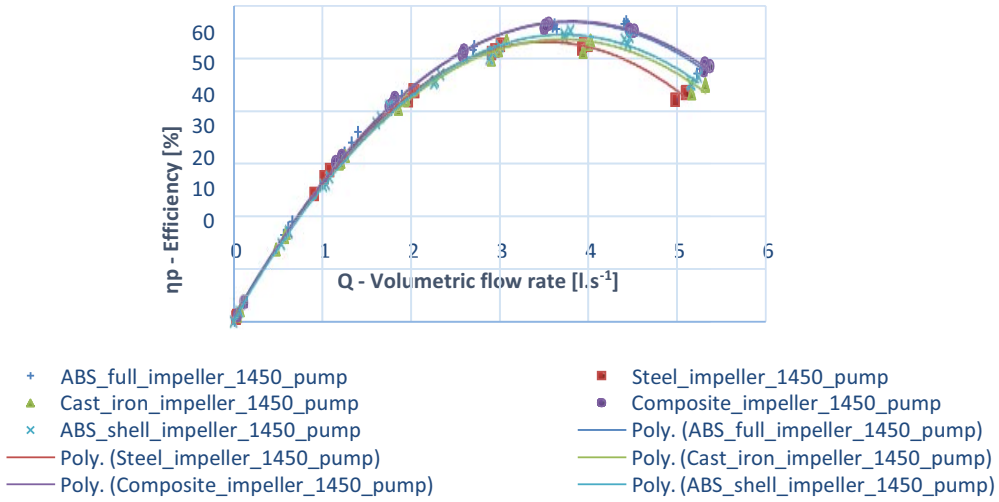

Figure 20. Pump efficiency vs flow rate

Pump mode power characteristics at 2,950 rpm.min^{-1} :

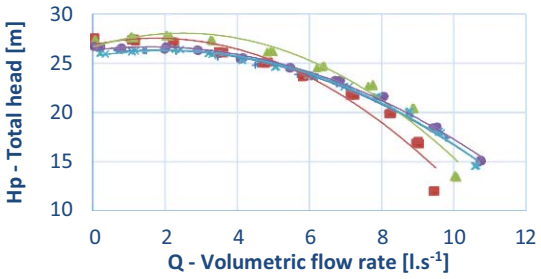

Figure 21. Total head vs flow rate

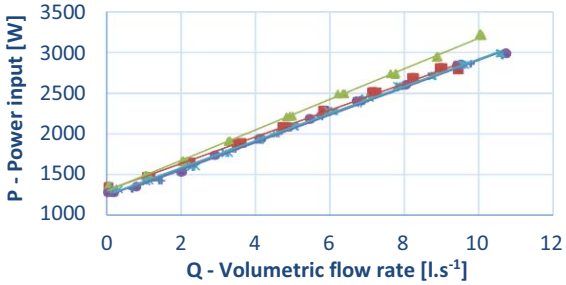

Figure 22. Power input vs flow rate

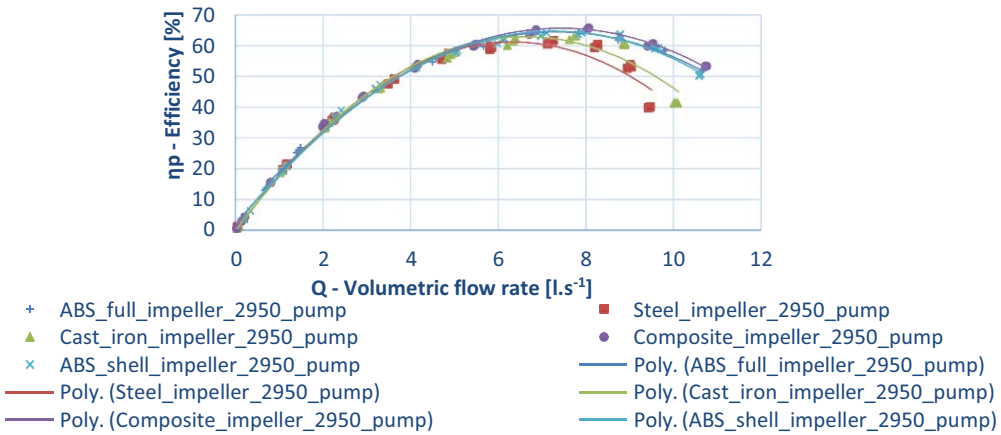

Figure 23. Pump efficiency vs flow rate

Turbine mode power characteristics:

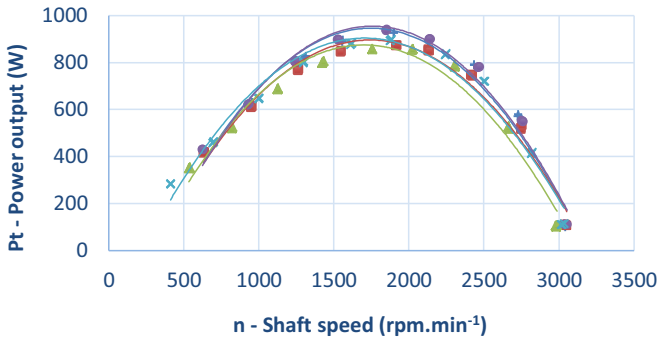

Figure 24. Mechanical power of the turbine vs shaft speed

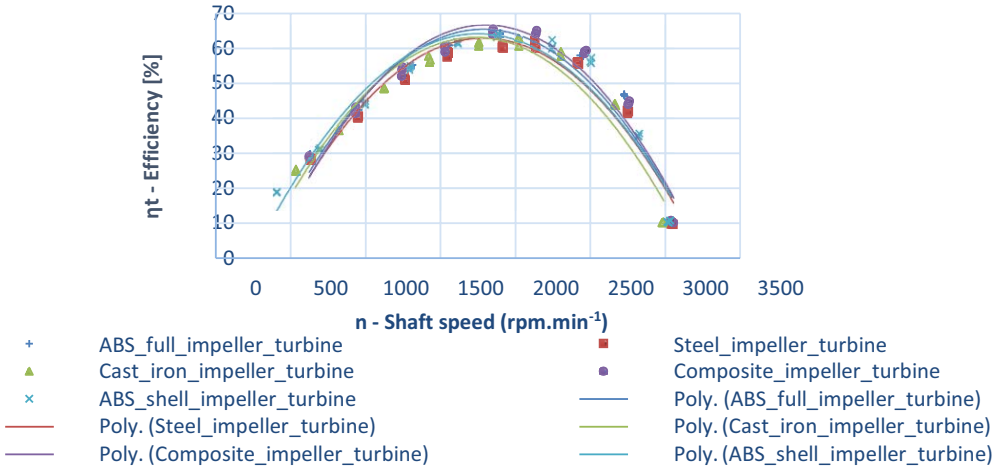

Figure 25. Turbine efficiency vs shaft speed

As in the reference, there is a good experience in achieving a higher quality (enamel) surface of prototypes during short-term soaking or exposure to the effects of acetone vapor or 1.2 dichloromethane. This often happens at the cost of reducing the strength of the component or losing shape and dimensional accuracy. The original intention was also to incorporate the adjustment in the production of impellers, but due to the shape-intensive geometry, the significantly different thicknesses of the components walls and the significant load in the verification tests in the hydraulic circuit. It was surrounded from this intention after several attempts. This is an issue for further independent work and for the repeatable use of these methods it is necessary to have the process properly tuned. The positive benefit of this treatment could be possible to prevent savories into the cavities of the wheels with liquid and thus avoid any mass imbalance. In the stress tests, it has been shown that although the wheels are capable of partially soaked with liquid, tests are of a short-term nature and minor intake had no effect on the course and test results. All variants of tested wheels have always endured high stress at full load in turbine and pump operation at 1,450 rpm.min^{-1} and 2,950 rpm.min^{-1} [7], [8].

Material tests of printed ABS at static tests on the tearing machine according ISO 527-1 and ISO 527-2 indicate a significant different of strong characteristic of samples printed in different directions of printing fibers. Strength properties should be taken into account already when designing the prototype itself, appropriately set the printing parameters due to the necessary time to print, consume materials and the purpose of the prototype, especially for mechanically strained prototypes.

5. Conclusions

The performance characteristics of the impellers tested and measured on the hydraulic circuit for the pump mode showed that all variants have very similar functional values to each other and very identical trends of functional curves of total head, power consumption and overall mechanical efficiency depending on flow compared to two operating conditions at 1,450 rpm.min^{-1} and 2,950 rpm.min^{-1}. The shapes of individual curves are almost identical, and values of the transport height and power correspond to the multiple of the speed of the operation. The total efficiency values of pumps in operation at a speed of 1,450 rpm.min^{-1} are around 52 % and in operation at a speed of 2,950 rpm.min^{-1} are around 62 %. The power characteristics of the impellers for the turbine mode show that all variants have also very similar functional values and very identical trends in functional curves of mechanical power and overall mechanical efficiency depending on speed. The values of the total mechanical efficiency of turbines are around 62 %, which corresponds to the type of operation. The characteristics of this turbine can be read from the measured values, where, at increasing speeds, the flow and overall efficiency grow up to the maximum of power and, with further increasing speed, the flow and efficiency decrease. In conclusion, the turbine achieves the highest performance and efficiency at optimum speeds.

Based on the experiments, prototypes produced by Rapid Prototyping technology achieve optimal values in hydraulic testing compared to conventionally produced impellers in both pump and turbine mode. While the choice of parameters in the processing of the virtual model, the quality of the material used and above all, the quality of 3D printing, plays a significant role. Following these boundaries conditions, this advanced technology can be successfully used in the verification of newly developed pumps, turbines and pump turbines.

Acknowledgements

The authors thanks to (a) the Internal Grant Agency 2020 of the Czech University of Life Sciences Prague for funding from the project of liquid flow analysis in hydrodynamic pump and pump in turbine mode, and (b) Atma Jaya Catholic University of Indonesia for the collaboration of the student exchange program.

References

[1] Pérez-Sánchez M, Sánchez-Romero F J, Ramos H M and López-Jiménez P A 2017 Energy recovery in existing water networks: Towards greater sustainability *Water* **9** (2) 97
[2] Li X, Chen B, Luo X and Zhu Z 2020 Effects of flow pattern on hydraulic performance and energy conversion characterisation in a centrifugal pump *Renewable Energy* **151** 475-487
[3] Han X, Kang Y, Li D and Zhao W 2018 Impeller optimized design of the centrifugal pump: A numerical and experimental investigation *Energies* **11** (6) 1444
[4] Mohan N, Senthil P, Vinodh S and Jayanth N 2017 A review on composite materials and process parameters optimisation for the fused deposition modelling process *Virtual and Physical Prototyping* **12** (1) 47-59
[5] Wickramasinghe S, Do T and Tran P 2020 FDM-based 3D printing of polymer and associated composite: A review on mechanical properties defects and treatments *Polymers* **12** (7) 1529
[6] Ramya A and Vanapalli S L 2016 3D printing technologies in various applications *International Journal of Mechanical Engineering and Technology* **7** (3) 396-409
[7] Kandananond K 2020 Optimization of fused filament fabrication system by response surface method *International Journal of Metrology and Quality Engineering* **11** 4
[8] Dave H K, Rajpurohit S R, Patadiya N H, Dave S J, Sharma K S, Thambad S S and Sheth K V 2019 Compressive strength of PLA based scaffolds: effect of layer height infill density and print speed *Int J Mod Manuf Technol* **11** (1) 21-7

[9] Höller S, Benigni H and Jaberg H 2019 Numerical and experimental investigation of the 4-Quadrant behavior of different mixed flow diffuser pumps *International Journal of Turbomachinery Propulsion and Power* **4** (1) 3
[10] Özkil A G 2017 Collective design in 3D printing: A large scale empirical study of designs designers and evolution *Design Studies* **51** 66-89
[11] Costa S F, Duarte F M and Covas J A 2015 Thermal conditions affecting heat transfer in FDM/FFE: a contribution towards the numerical modelling of the process: This paper investigates convection conduction and radiation phenomena in the filament deposition process *Virtual and Physical Prototyping* **10** (1) 35-46
[12] Garg A, Bhattacharya A and Batish A 2016 On surface finish and dimensional accuracy of FDM parts after cold vapor treatment *Materials and Manufacturing Processes* **31** (4) 522-529
[13] Stergiou G S, Alpert B, Mieke S, Asmar R, Atkins N, Eckert S and O'Brien E 2018 A universal standard for the validation of blood pressure measuring devices: Association for the Advancement of Medical Instrumentation/European Society of Hypertension/International Organization for Standardization Collaboration Statement Hypertension **71** (3) 368-374
[14] Iso E 2012 *Plastics—Determination of tensile properties—Part 1: General principles* Geneva Switzerland: International Organization of Standardization
[15] Polák M 2017 Experimental evaluation of hydraulic design modifications of radial centrifugal pumps *Agron. Res* **15** 1189-1197
[16] Polák M 2019 The influence of changing hydropower potential on performance parameters of pumps in turbine mode *Energies* **12** (11) 2103